

Temperature of the QGP: a brief overview

Mike Sas

Wright Laboratory, Yale University, New Haven CT, USA

Received 3 July 2022; accepted 15 September 2022

These proceedings give a brief overview of the measurements of the effective temperature of the quark-gluon plasma.

Keywords: Temperature, quark-gluon plasma, electromagnetic probes

1 Introduction

The quark gluon plasma is a strongly coupled state of matter that is formed by the overlapping nucleons of two colliding heavy-ions[1]. In the overlap region the thermodynamic properties of the colliding matter, such as temperature, pressure, and energy density, are so large that a phase transition into this extraordinary type of matter occurs. After its creating the QGP will expand, cool down, and its constituents will hadronize into ordinary matter. Here, the temperature plays an important role in understanding the space-time dynamics of the QGP evolution, as the hydrodynamical description of the QGP phase uses an equation of state that depends on T, p, ϵ [2–4].

The temperatures reached in these collisions at RHIC and the LHC is estimated to be of the order of 300 MeV, well above the pseudo-critical temperature of 150 MeV which has been calculated by lattice QCD [1]. There are two conceptually different approaches that tell us more about the temperature, which are either data or model driven. First, the slope of the transverse momentum spectra of thermal photons and dileptons is related to the temperature of the system. Since these thermal probes are created all throughout the evolution of the QGP, this measurement relates to the effective temperature of the system (T_{eff}). Secondly, state-of-the-art theoretical calculations, employing Bayesian inference, use a whole collection of hadronic data and are able to provide posterior distributions of a set of parameters that describe the QGP[5]. These parameters are then either important for the initial and early state, as well as the evolution of the hydrodynamical phase. The temperature of the system is usually not one of the parameters constrained by this method, but can be calculated at any point in the space-time evolution of the system.

In these proceedings brief overview is given from both the experimental and theoretical side, concluded by a discussion on possible future steps to get a better understanding.

2 Theoretical overview

In dynamical model calculations of the QGP, the temperature can be calculated for each fluid element at any point in time during the evolution. This calculation is done by obtaining the local energy density from the stress tensor, which via the equation of state is related to the temperature T . Here, it is then possible to calculate several different temperatures, such

as the fluid element with the maximum available temperature T_{max} and the average temperature $\langle T \rangle$, all at a specific time (τ). It is important to note that the fluctuations of the entropy density of the initial state lead to large local temperature differences at early times. Furthermore, as the colliding nuclei have a nuclear thickness that is larger toward its center, more central AA collisions create initial states with larger entropy densities compared to more peripheral collisions. A detailed calculation of T_{max} and $\langle T \rangle$ as function of collision centrality has been performed using the Trajectum code, as shown in Figure 1 [5]. The time at which the temperature is evaluated is $\tau = 1.17 \text{ fm}/c$, coinciding with the time the hydrodynamical phase starts for this specific model calculation. T_{switch} is the temperature at which the model stops the hydrodynamical evolution and starts the hadronization process. The result shows a clear collision centrality dependence, with central collisions being significantly hotter than peripheral ones.

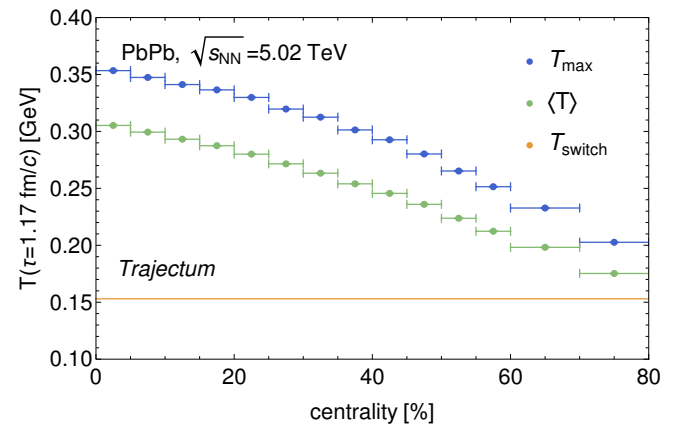


FIGURE 1. Centrality dependence of the temperatures T_{max} and $\langle T \rangle$ at $\tau = 1.17 \text{ fm}/c$, as calculated using Trajectum.

Experimentally we can access the temperature by measuring thermal photons that are emitted by the hot plasma[6–10]. By incorporating thermal photon production in the hydrodynamical phase of a model calculation, one is then able to try to relate the temperature to the spectrum of thermal photons that results from the QGP. Some of the model calculations also include thermal photons from the pre-equilibrium stage as well as the hadron gas. The thermal photon production rate depends on the local fluid properties such as the fluid

four-vector and the temperature. The total yield of these thermal photons can be calculated as an integral over the space-time volume of the medium, which depends on the size and the lifetime of the system as

$$\frac{d^4 N_{\gamma, \text{direct}}}{d^4 k} = \int d^4 X \frac{d^4 \Gamma_{\gamma, \text{direct}}}{d^4 k}(K^\mu, u^\mu(X), T(X)),$$

where $\Gamma_{\gamma, \text{direct}}$ is the thermal photon production rate, which depends on its four-vector K^μ , flow velocity $u^\mu(X)$, and temperature of the thermal system $T(X)$. The instantaneous rate is the largest at early times when the system is at its highest temperature, which goes down for later times when the system is expanding and cooling down. Interestingly, the total rate of thermal photons tends to increase as time progresses, as the volume of the system rapidly increases while the temperature remains relatively high [11]. This implies temperature measurements are perhaps more sensitive to late times, as here the majority of photons are produced.

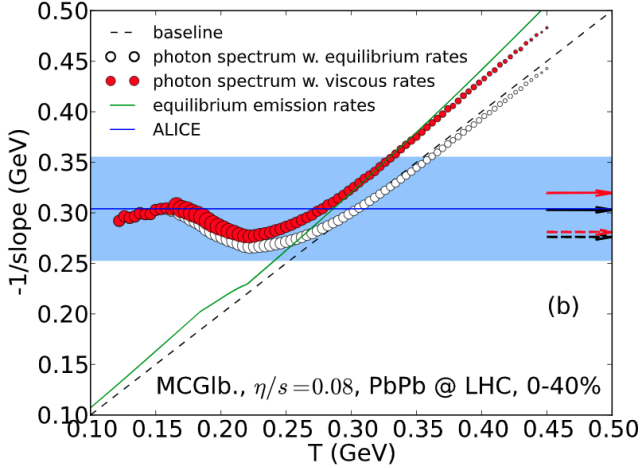


FIGURE 2. The inverse slope parameter $-1/\text{slope} = T_{\text{eff}}$ as function of temperature T as calculated in a hydrodynamical model. The blue band indicates the T_{eff} as measured by ALICE at $\sqrt{s_{\text{NN}}} = 2.76$ TeV.

The shape or slope of the thermal photon spectrum, which is as function of transverse momentum p_T , depends on the temperature of the QGP. A hotter plasma is able to emit higher p_T thermal photons compared to colder plasmas. Also, these spectra are a sum of the photons emitted all throughout the evolution of the system and are blueshifted due the radially expanding emission points within the plasma. Even if there are these complications, it is common to fit the thermal photon spectrum with $A \cdot e^{-p_T/T_{\text{eff}}}$, where T_{eff} is the effective temperature of the system. Figure 2 shows a hydrodynamical calculation where the T_{eff} is plotted for different temperatures of the QGP. At early times where the temperature is high, the $T_{\text{eff}} \sim T$, after which it starts to depart more from the baseline towards later times, which is the impact from radial flow. The size of the data points are related to the yield of the photons at that time, also indicating that most

photons are emitted rather late during the evolution. The ALICE measurement of $T_{\text{eff}} = 297 \pm 12^{\text{stat}} \pm 41^{\text{sys}}$ is similar to what the model calculation shows.

3 Experimental overview

In experiments it is not a priori known which photon is produced as thermal radiation from the plasma, especially considering the vast amount of photons coming from neutral meson decays. Therefore, one of the common methods is to subtract the decay photons on statistical basis from the distribution of inclusive photons, where first the excess of direct photons is measured via the p_T dependent double ratio

$$R_\gamma \equiv \frac{\gamma_{\text{incl}}}{\pi_{\text{param}}^0} / \frac{\gamma_{\text{decay}}}{\pi_{\text{param}}^0} = \frac{\gamma_{\text{incl}}}{\gamma_{\text{decay}}},$$

where γ_{incl} and γ_{decay} are the inclusive and decay photon yields, respectively, and π_{param}^0 a parametrization of the measured π^0 spectrum. Then, the direct yield can be calculated using

$$\gamma_{\text{direct}} = \gamma_{\text{incl}} - \gamma_{\text{decay}} = \left(1 - \frac{1}{R_\gamma}\right) \cdot \gamma_{\text{incl}}.$$

This approach has been used at both RHIC and the LHC, at various beam energies and collision systems. Figure 3 shows the double ratio R_γ and direct photon yield as function of p_T for different collision centralities as measured in ALICE at $\sqrt{s_{\text{NN}}} = 2.76$ TeV [12]. The R_γ at the LHC is only slightly above unity at lower p_T and is consistent with pQCD calculations of prompt photons at higher p_T . The resulting direct photon yields agree with the hydrodynamical calculations, and are fitted at lower p_T to estimate T_{eff} . Similar measurements are performed at RHIC, both utilizing calorimetric and conversion photon reconstruction techniques, as well as measurements of thermal dileptons. A compilation of the effective temperatures as function of $\sqrt{s_{\text{NN}}}$ is shown in Figure 4, which fits the corresponding direct photon yields for different p_T ranges [13]. Interestingly, it seems that T_{eff} is similar for each beam energy as long as the same integration range is used.

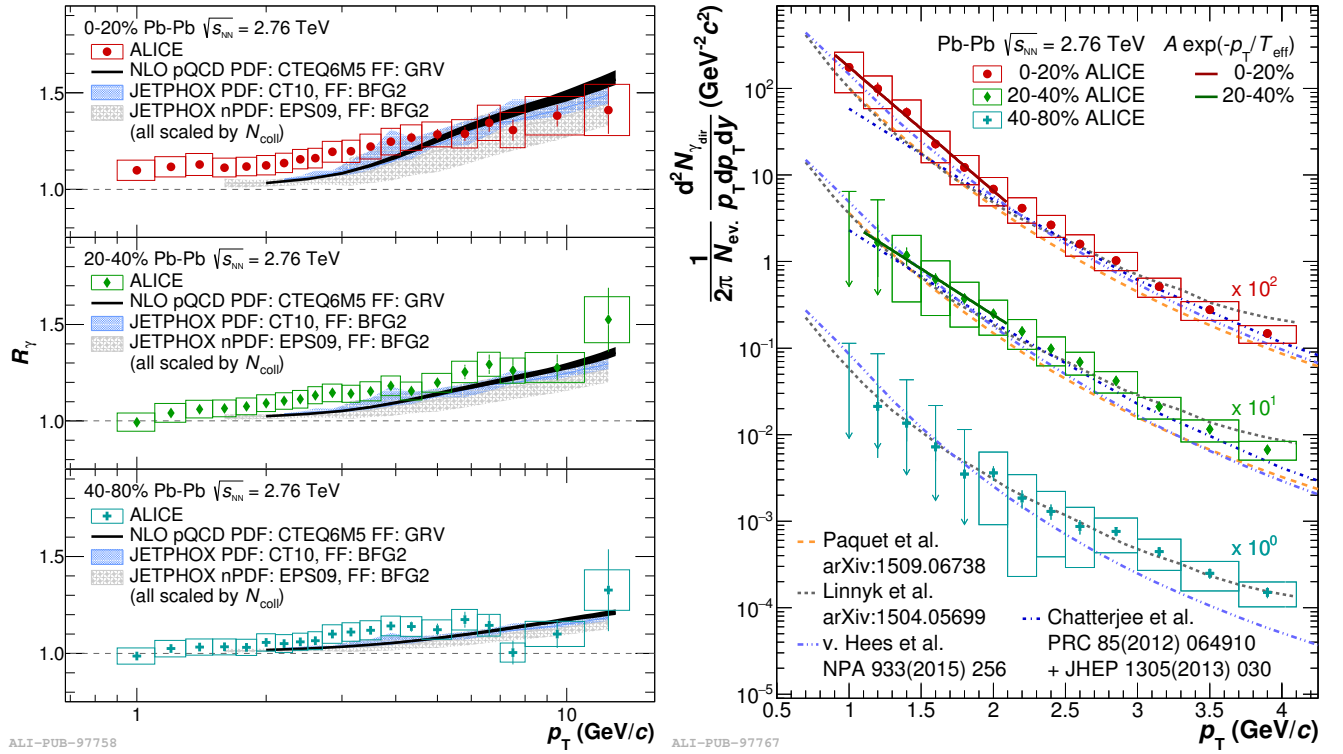


FIGURE 3. Double ratio R_γ and direct photon yield as function of p_T for different collision centralities as measured in ALICE at $\sqrt{s_{NN}} = 2.76$ TeV [12].

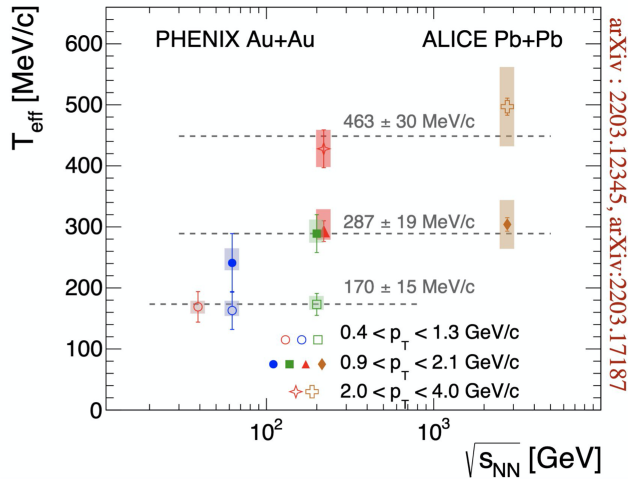


FIGURE 4. The effective temperature as function of $\sqrt{s_{NN}}$, calculated from the direct photon yields measured at RHIC (PHENIX) and the LHC (ALICE) [13].

4 Discussion

These proceedings give a brief overview of the measurements of the effective temperature of the quark-gluon plasma. With temperatures around 300 MeV it implies that we are deal-

ing with a system well above the pseudo-critical temperature of 150 MeV as predicted by lattice QCD. However, it remains a challenging experiment as the signal is so dominated by photons produced in neutral meson decays in the case of real photons, as well as the large backgrounds of dileptons in the case of virtual photons. In addition, the direct photon yields as measured in experiment are summing the photons produced by the hot plasma over the entire space-time evolution of the system, such that the slope of the spectrum only relates to the effective temperature T_{eff} . In addition, the measurements of T_{eff} show that there is a p_T dependence, which is not expected from the thermal photon yields from theoretical models. It would be interesting to find out whether the p_T dependence of T_{eff} could put limits on photons coming from the pre-equilibrium phase or perhaps the hadron gas. Similarly, state-of-the-art model calculations, for example those that use Bayesian inference to constrain QGP parameters, can be used to investigate the relationship between the temperature evolution of the system with respect to the amplitude of T_{eff} .

Special thanks go out to Govert Nijs and Wilke van der Schee, for discussions and providing calculations, and to Klaus Reygers for many discussions about the QGP temperature. This work was supported in part by the Office of Nuclear Physics of the U.S. Department of Energy. Work supported by the US DOE under award number DE-SC004168.

-
1. Wit Busza, Krishna Rajagopal, and Wilke van der Schee. Heavy Ion Collisions: The Big Picture, and the Big Questions. *Ann. Rev. Nucl. Part. Sci.*, 68:339–376, 2018. doi: 10.1146/annurev-nucl-101917-020852.
 2. A. Bazavov et al. Equation of state and QCD transition at finite temperature. *Phys. Rev. D*, 80:014504, 2009. doi: 10.1103/PhysRevD.80.014504.
 3. Owe Philipsen. The QCD equation of state from the lattice. *Prog. Part. Nucl. Phys.*, 70:55–107, 2013. doi: 10.1016/j.pnpnp.2012.09.003.
 4. A. Bazavov et al. Equation of state in (2+1)-flavor QCD. *Phys. Rev. D*, 90:094503, 2014. doi: 10.1103/PhysRevD.90.094503.
 5. Govert Nijs, Wilke van der Schee, Umut Gürsoy, and Raimond Snellings. Bayesian analysis of heavy ion collisions with the heavy ion computational framework trajectory. *Physical Review C*, 103(5), may 2021. doi: 10.1103/physrevc.103.054909. URL <https://doi.org/10.1103%2Fphysrevc.103.054909>.
 6. P.V. Ruuskanen. Electromagnetic probes of quark - gluon plasma in relativistic heavy ion collisions. *Nucl. Phys. A*, 544:169–182, 1992. doi: 10.1016/0375-9474(92)90572-2.
 7. Simon Turbide, Charles Gale, Evan Frodermann, and Ulrich Heinz. Electromagnetic radiation from nuclear collisions at RHIC energies. *Phys. Rev. C*, 77:024909, 2008. doi: 10.1103/PhysRevC.77.024909.
 8. Jean-François Paquet, Chun Shen, Gabriel S. Denicol, Matthew Luzum, Björn Schenke, Sangyong Jeon, and Charles Gale. Production of photons in relativistic heavy-ion collisions. *Phys. Rev. C*, 93(4):044906, 2016. doi: 10.1103/PhysRevC.93.044906.
 9. Jean-François Paquet. Overview of electromagnetic probe production in ultra-relativistic heavy ion collisions. *J. Phys. Conf. Ser.*, 832(1):012035, 2017. doi: 10.1088/1742-6596/832/1/012035.
 10. Chun Shen. Electromagnetic Radiation from QCD Matter: Theory Overview. *Nucl. Phys. A*, 956:184–191, 2016. doi: 10.1016/j.nuclphysa.2016.02.033.
 11. Chun Shen, Ulrich W Heinz, Jean-Francois Paquet, and Charles Gale. Thermal photons as a quark-gluon plasma thermometer reexamined. *Phys. Rev. C*, 89(4):044910, 2014. doi: 10.1103/PhysRevC.89.044910.
 12. Jaroslav Adam et al. Direct photon production in Pb-Pb collisions at $\sqrt{s_{NN}} = 2.76$ TeV. *Phys. Lett.*, B754: 235–248, 2016. doi: 10.1016/j.physletb.2016.01.020.
 13. PHENIX collaboration. Low- p_t direct-photon production in au+au collisions at $\sqrt{s_{NN}} = 39$ and 62.4 gev, 2022. URL <https://arxiv.org/abs/2203.12354>.